



Limitation of the transport capacity approach in sediment transport modeling

G. C. Sander,¹ J.-Y. Parlange,² D. A. Barry,³ M. B. Parlange,³ and W. L. Hogarth⁴

Received 15 May 2006; revised 14 August 2006; accepted 8 September 2006; published 6 February 2007.

[1] In a recent paper by Polyakov and Nearing (2003) it was shown experimentally that the sediment transport capacity in a rill is not unique for a given soil type, slope, and flow rate. Indeed, they found that the transport capacity was dependent on whether sediment transport in the rill was occurring under net erosion or net deposition conditions. They concluded that this nonuniqueness in transport capacity is a discrepancy that needs addressing in soil erosion models. Here we postulate that this behavior occurs as a result of defining transport capacity as an model input to distinguish between net erosion and net deposition regimes, instead of determining it as an outcome between the separate but continuous rate processes of deposition and entrainment such as is the case for the multisize class erosion model of Hairsine and Rose (1992a, 1992b). This model is used to reinterpret and reproduce the results of Polyakov and Nearing (2003). The analysis shows that the transport capacity cannot be unique for a soil composed of a range of size classes and that uniqueness only occurs for the exceptional case of single size class soil. Consequently, when used as a model input, the transport capacity concept is deficient in modeling sediment transport of real soils across different flow conditions.

Citation: Sander, G. C., J.-Y. Parlange, D. A. Barry, M. B. Parlange, and W. L. Hogarth (2007), Limitation of the transport capacity approach in sediment transport modeling, *Water Resour. Res.*, 43, W02403, doi:10.1029/2006WR005177.

1. Introduction

[2] Nearly all commonly used process-based erosion models such as ANSWERS [Beasley *et al.*, 1980], EUROSEM [Morgan *et al.*, 1998], KINEROS [Woolhiser *et al.*, 1990], LISEM [De Roo *et al.*, 1996] and WEPP [Nearing *et al.*, 1989] adopt the concept of transport capacity to distinguish between sediment transport occurring within net eroding or net depositional regimes. For one-dimensional steady state sediment transport in a rill in the absence of rainfall, these models are essentially given by

$$\frac{dq_s}{dx} = D_r, \quad (1)$$

where x is the distance along the rill (m), $q_s = qc$ is the sediment flux or load ($\text{kg m}^{-1} \text{s}^{-1}$), q is the water flux ($\text{m}^2 \text{s}^{-1}$), c is the sediment concentration (kg m^{-3}) and D_r is the rill sediment source term defined as

$$D_r = \alpha(1 - q_s/T_c) \quad (2)$$

for net erosion ($D_r > 0$) or

$$D_r = \frac{v_f}{q}(T_c - q_s) \quad (3)$$

for net deposition ($D_r < 0$). In (2) and (3), T_c is the transport capacity ($\text{kg m}^{-1} \text{s}^{-1}$), α is an empirical constant [Polyakov and Nearing, 2003] and v_f is the effective fall velocity (m s^{-1}). In this model T_c is a predefined input that distinguishes between net erosion and net deposition conditions.

[3] A consequence of having two different equations for D_r is that while it is a continuous function of the sediment flux, the change in D_r with q_s or dD_r/dq_s is discontinuous at $q_s = T_c$. However, there is nothing in the transition from a net eroding to a net depositing flow condition that would give rise to this discontinuity. Physically, it is a smooth transition, and erosion models should reflect this behavior.

[4] The only erosion model that considers deposition as a separate rate process was developed by Hairsine and Rose [1992a, 1992b]. Their model incorporates a multiparticle size class description of sediment transport to account for the preferential deposition of suspended sediment due to gravity. Consequently, it also incorporates the formation and evolution of a covering layer of deposited sediment which has a different cohesive strength to the original uneroded soil. In their model the transport capacity of the flow is determined as a limiting outcome of the evolution of the dynamic balance between the individual deposition and erosion processes. Conditions of net erosion and net deposition are merely a change in the balance of these processes. In the absence of rainfall-driven erosion, the steady state

¹Department of Civil and Building Engineering, Loughborough University, Loughborough, UK.

²Department of Biological and Environmental Engineering, Cornell University, Ithaca, New York, USA.

³School of Architecture, Civil and Environmental Engineering, Ecole Polytechnique Fédérale de Lausanne, Lausanne, Switzerland.

⁴Faculty of Science and Information Technology, University of Newcastle, Newcastle, New South Wales, Australia.

equations of the Hairsine-Rose model for suspended sediment are given by

$$\frac{dq_{si}}{dx} = r_i + r_{ri} - d_i, \quad i = 1, 2, \dots, I \quad (4)$$

$$\frac{\partial m_i}{\partial t} = d_i - r_{ri}, \quad i = 1, 2, \dots, I, \quad (5)$$

where t is time (s), I is the number of particle size classes, i is a counter denoting size class with $i = 1$ being the smallest, $q_{si} = qc_i$ is the sediment load of each size class, c_i is the sediment concentration in each class, r_i is the entrainment rate of original soil in each size class ($\text{kg m}^{-2} \text{s}^{-1}$), d_i is the deposition rate of suspended sediment in size class i ($\text{kg m}^{-2} \text{s}^{-1}$), r_{ri} is the reentrainment rate of deposited sediment ($\text{kg m}^{-2} \text{s}^{-1}$) and m_i is the mass of sediment of size class i in the deposited layer (kg m^{-2}). The total suspended sediment concentration, c , and total mass in the deposited layer, m_t , is then found by summing across all size classes as $c = \sum_{i=1}^I c_i$ and $m_t = \sum_{i=1}^I m_i$.

[5] The erosion source and sink terms in (4) and (5) are expressed as [Hairsine and Rose, 1992b]

$$r_i = p_i(1-H)\frac{F}{J}(\Omega - \Omega_{cr}), \quad (6)$$

$$r_{ri} = H\frac{F}{gh}\left(\frac{\rho_s}{\rho_s - \rho}\right)(\Omega - \Omega_{cr})\frac{m_i}{m_t}, \quad (7)$$

$$d_i = v_i c_i, \quad (8)$$

in which p_i ($0 < p_i \leq 1$ and $\sum_{i=1}^I p_i = 1$) is the proportion of sediment in size class I of the original uneroded soil, H ($0 \leq H \leq 1$) is the protection factor given by the deposited layer, F is the fraction of excess stream power which is effective in entrainment (approximately 0.1–0.2 [Proffitt et al., 1993]), J (J kg^{-1}) is the experimentally determined specific energy of entrainment, g is the acceleration due to gravity, ρ and ρ_s are the water and sediment densities respectively, h is the flow depth in the rill, v_i are the fall velocities for each size class (m s^{-1}), Ω (W m^{-2}) = $\rho g S_o Q / W_b = \rho g S_o q$ is the stream power with Ω_{cr} the critical threshold stream power, S_o is the rill slope, Q the volumetric flow rate ($\text{m}^3 \text{s}^{-1}$) and W_b the base width of the rill. The rills are assumed to be rectangular for calculating hydraulic flow properties [Polyakov and Nearing, 2003].

[6] The Hairsine-Rose model has two different steady state solutions for the c_i . The first of these occurs for a zero sediment concentration at the $x = 0$ boundary, as given by Hairsine and Rose [1992a], and results in the m_i also achieving steady state. The second is for $c_i(x = 0) \neq 0$ as given by Beuselinck et al. [2002a, 2002b], Hairsine et al. [2002] and Sander et al. [2002], in which case the m_i do not reach steady state but increase with time. The first case corresponds to net erosion conditions while the second is for net deposition conditions. In this paper we will use both

of these solutions to reinterpret some recent and precise experiments by Polyakov and Nearing [2003]. In addition we show that the Hairsine-Rose model provides the explanation of the nonuniqueness in transport capacity between net erosional and net depositional flows, and that a unique transport capacity can only occur for soils which are only composed of a single size class.

2. Solutions of Hairsine-Rose Model for Net Erosion and Net Deposition Conditions

[7] As a result of the ongoing deposition process, the deposited sediment in the rill will provide a proportion of cover H to the original soil. Complete protection or coverage of the original soil bed, so that only previously eroded sediment is being transported, is given by $H = 1$. Thus under steady state conditions the value of H also differentiates between a net erosion ($H < 1$) or a net deposition ($H = 1$) regime. In the solutions presented below we assume that the volumetric flow rate through the rill and the width of the rill remain constant. Flow data in Table 2 of Polyakov and Nearing [2003] support this approximation.

2.1. Net Erosion $c(x = 0) = 0$

[8] For the net erosion experiments $H < 1$ and the deposited layer will reach steady state, thus $\partial m_i / \partial t = 0$. Following Sander et al. [1996] we take

$$H = \frac{m_t}{m_t^*}, \quad (9)$$

where m_t^* is the mass of sediment in the deposited layer required to completely shield the original soil. For a constant flow depth and water flux we define the constants

$$\lambda = \frac{F}{J}(\Omega - \Omega_{cr}) \quad (10)$$

$$\gamma = \frac{F}{gh}\left(\frac{\rho_s}{\rho_s - \rho}\right)(\Omega - \Omega_{cr}), \quad (11)$$

then from (5), (7) and (8), at steady state

$$\frac{m_i}{m_t^*} = \frac{v_i c_i}{\gamma}. \quad (12)$$

Summing (12) over i gives $H = \gamma^{-1} \sum_{i=1}^I v_i c_i$ and from (4) and (6)

$$\frac{dc_i}{dx} = \frac{p_i \lambda}{q} \left(1 - \frac{1}{\gamma} \sum_{i=1}^I v_i c_i\right), \quad i = 1, 2, \dots, I. \quad (13)$$

If we take the ratio of (13) for any two size classes, in particular i and I , then we obtain the equation

$$\frac{dc_i}{dc_I} = \frac{p_i}{p_I}, \quad (14)$$

which has the solution

$$c_i(x) = \frac{p_i}{p_I} c_I(x), \quad i = 1, 2, \dots, I - 1. \quad (15)$$

Solutions for all size classes are therefore simply given as a proportion of the largest size class. Substituting for c_i from (15) into (13) and integrating subject to the condition $c_I(x=0) = 0$, gives

$$c_I(x) = p_I \frac{\gamma}{\sum_{i=1}^I p_i v_i} \left[1 - \exp \left(- \frac{\lambda \sum_{i=1}^I p_i v_i}{\gamma q} x \right) \right]. \quad (16)$$

Summing across all size classes in (15) gives the total concentration in suspension as

$$\begin{aligned} c(x) &= \frac{c_I(x)}{p_I} \\ &= \frac{\gamma}{\sum_{i=1}^I p_i v_i} \left[1 - \exp \left(- \frac{\lambda \sum_{i=1}^I p_i v_i}{\gamma q} x \right) \right], \end{aligned} \quad (17)$$

which has the same form as (2) of *Polyakov and Nearing* [2003], i.e., $c(x) = (T_c/q)[1 - \exp(-\alpha x/T_c)]$. Comparing this expression with the corresponding solution of the Hairsine-Rose model as given by (17) shows similarity in form, and are identical if

$$T_c = \frac{q\gamma}{\sum_{i=1}^I p_i v_i} \quad (18)$$

$$\alpha = \lambda. \quad (19)$$

2.2. Net Deposition $c(x=0) \neq 0$

[9] For the net deposition experiments $H=1$ and thus $r_i=0$. Consequently, m_i in the deposited layer will not reach steady state and $\partial m_i/\partial t \neq 0$ as mentioned above. However, since c_i does achieve steady state then it is clear from (4) and (7) that it is the ratio m_i/m_t which reaches equilibrium. The solution of the Hairsine-Rose model under these conditions was given recently by *Sander et al.* [2002] as

$$c_i(x) = c_i(0) \left[\frac{c_I(x)}{c_I(0)} \right]^{v_i/v_I}, \quad i = 1, 2, \dots, I-1, \quad (20)$$

$$\int_{c_I(0)}^{c_I} \left[\frac{\gamma}{\sum_{i=1}^I v_i c_i(0) [\bar{c}_I/c_I(0)]^{v_i/v_I}} - 1 \right]^{-1} \frac{d\bar{c}_I}{\bar{c}_I} = \frac{v_I}{q} x, \quad (21)$$

$$m_i(x, t) \simeq v_i c_i(x) \left[1 - \gamma / \sum_{i=1}^I v_i c_i(x) \right] t + \dots, \quad i = 1, 2, \dots, I, \quad (22)$$

where $c_i(0)$ are the incoming concentrations for each size class at $x=0$. Note that (22) corresponds to the leading

order term for asymptotic behavior in m_i as $t \rightarrow \infty$. The transport capacity is found for net deposition conditions from (20) as

$$T_c = q \sum_{i=1}^I c_i(\infty) = q \sum_{i=1}^I c_i(0) \left[\frac{c_I(\infty)}{c_I(0)} \right]^{v_i/v_I}, \quad (23)$$

with $c_I(\infty)$ found from (21) for $dc_I/dx = 0$ with $x \rightarrow \infty$ as

$$\sum_{i=1}^I v_i c_i(0) [c_I(\infty)/c_I(0)]^{v_i/v_I} = \gamma. \quad (24)$$

Note that it is only for $x \rightarrow \infty$ does $m_i = 0$ to leading order in (22). For $x < \infty$, $c_i(x) > c_i(\infty)$, and $\gamma = \sum v_i c_i(\infty)$ is $< \sum v_i c_i(x)$ and m_i is > 0 .

3. Results and Discussion

[10] *Polyakov and Nearing* [2003] performed a precise set of experiments to study “whether sediment transport capacity is a unique value for [a] given soil, flow rate and slope, and to determine if equilibrium sediment concentration in the rill obtained by detachment was different from that observed under depositional conditions.” These experiments covered four scenarios; that is, two different volumetric flow rates of 6 and 9 L min⁻¹ were applied at the top of the rill with the incoming water being either clear or heavily laden with sediment. This gave two data sets for net erosion conditions (clear inflowing water) and two data sets for net deposition conditions (sediment laden inflow). Sediment concentrations were then measured at different distances down the rill with a maximum distance of 8 m. The experimental data showed that the transport capacity was not unique and different values were obtained for the net erosion and net deposition conditions.

3.1. Parameter Determination and Predictions

[11] To apply the Hairsine-Rose model to their data, we need to determine values for the settling velocities v_i , size class proportions p_i , incoming concentrations $c_i(x=0)$ for the added sediment experiments, depth of flow in the rill h and rectangular rill width W_b , plus flow parameters λ and γ as specified in (10) and (11). Values of all parameters are given in Tables 1 and 2. Note that soil parameters p_i and v_i are taken to be the same for all experiments while the other parameters depend on flow conditions.

[12] Table 1 of *Polyakov and Nearing* [2003] provides values of $c_i(x=2, 8 \text{ m})$ for five ($I=5$) size classes. For the no added sediment experiment the measured $c_i(x)$ data allow p_i to be found through (15) by

$$p_i = \frac{c_i(x)}{\sum_{i=1}^I c_i(x)}.$$

Values of p_i calculated from the $x=2$ or 8 m data from both the $Q=6$ or 9 L min⁻¹ flow rates showed very little variation. The values given in Table 1 were calculated by averaging the $x=2$ and 8 m data for $Q=6$ L min⁻¹, i.e., $p_i = [p_i(x=2) + p_i(x=8)]/2$. In Table 2 we give the average rill flow parameters for all experiments from *Polyakov and*

Table 1. Soil Parameters and the Added Sediment Experiments Inflow Concentrations for $Q = 6$ and 9 L min^{-1}

p_i	$v_i, \text{ m s}^{-1}$	$c_i(0), \text{ kg m}^{-3}$	
		$Q = 6$	$Q = 9$
0.376	0.0038	38.7	62.7
0.234	0.0137	24.1	39.1
0.2	0.0827	20.6	33.4
0.166	0.1369	17.1	27.8
0.0237	0.2317	2.5	4.0

Nearing [2003]. It is clear that the hydraulic flow properties h , W_b and q of the rill are slightly different for each experiment and consequently the flow parameters γ and λ are expected to vary for each of the four experiments.

[13] Determining the boundary concentrations $c_i(0)$ for the net deposition experiments and the settling velocities requires some care. The reported data are provided not for each size class $c_i(0)$ but for all size classes $c(0)$, being 103 kg m^{-3} and 167 kg m^{-3} for $Q = 6$ and 9 L min^{-1} respectively. A straightforward approach is to assume that $c(0)$ is spread across the size classes in accordance with p_i , i.e., $c_i(0) = p_i c(0)$. Polyakov and Nearing [2003], state that “air dried sediments were added to the flow” and as a result of the air drying “this probably ... caused flaking due to rapid wetting and, as a consequence, reduction in aggregate size ... complicating the comparison of sediment aggregate sizes between the two regimes.” While this suggests that the inflowing concentrations have more than likely been perturbed from $p_i c(0)$, they are still the best available estimate and are given in Table 1. The $c_i(0)$ for the higher flow rate were obtained by simply multiplying the lower flow rate values by the factor 167/103.

[14] Experimental data were provided on particle diameters via sieve size. To convert these to a settling velocity distribution we use (9) of Cheng [1997]

$$\frac{v_i s_i}{w} = \left(\sqrt{25 + 1.2s_*^2} - 5 \right)^{3/2} \quad (25)$$

$$s_* = \left[\frac{(\rho_s - \rho)g}{\rho w^2} \right]^{1/3} s_i,$$

where w is the kinematic viscosity (0.001 m s^{-1}) and s_i is the sieve diameter. Using the sieve diameters of 0.1, 0.21, 1, 2 and 4.76 mm from Table 4 of Polyakov and Nearing [2003] results in the fall velocities shown in Table 1.

[15] For the no added sediment experiments Polyakov and Nearing [2003] give $T_c/q = 36.2 \text{ kg m}^{-3}$ and $\alpha/T_c = 0.243 \text{ m}^{-1}$ for $Q = 6 \text{ L min}^{-1}$ and $T_c/q = 54.4 \text{ kg m}^{-3}$, and $\alpha/T_c = 0.364 \text{ m}^{-1}$ for $Q = 9 \text{ L min}^{-1}$, allowing γ and λ to be determined from (18) and (19) given that p_i and v_i are known. For the sediment added experiments γ is calculated from (24). Finally, taking $\rho_s = 2000 \text{ kg m}^{-3}$ and $\rho = 1000 \text{ kg m}^{-3}$ (10) and (11) can then be rearranged to provide values for J and $F(\Omega - \Omega_{cr})$. From the data given it is possible to calculate the stream power Ω in each experiment, noting that the bed slope was 7% [Polyakov and Nearing, 2003]. While Ω_{cr} seems not available, a typical value for cultivated soil is 0.007 W m^{-2} which allows F to be estimated as

shown in Table 2. Thus the values of F derived for these experiments are entirely consistent with the values obtained by others, such as Proffitt *et al.* [1993]. The parameter J only occurs in the entrainment source term r_i and since the steady state net deposition experiments result in the original soil being completely covered by deposited sediment then $H = 1$ and $r_i = 0$. Consequently, the sediment added steady state data set does not allow for J to be calculated directly.

[16] A comparison between the measured experimental data of Polyakov and Nearing [2003] and the predictions of the Hairsine-Rose model for the total steady state sediment concentration is shown in Figures 1 and 2. Comparisons between measured and predicted concentrations for the individual size classes for both the net deposition and net erosion experiments are found in Table 3. Predictions for the no added sediment are obtained from (15) to (17), while those for added sediment are found from (20), (21) and (24). Clearly, the ability of the Hairsine-Rose model to capture the behavior of all the size classes across the entire of experimental flow conditions is remarkable. Matching the sediment concentrations of individual size classes is far more difficult than matching total concentrations. The results in Table 3 show that the Hairsine-Rose model has been able to achieve this level of matching for both erosion regimes and therefore provides compelling evidence for the physical applicability of the conceptual approach adopted in their model.

[17] Figures 3 and 4 show the mass contribution of the different particle sizes to the deposited layer as a function of distance down the rill when transport is occurring under, respectively, net erosion and net deposition regimes. In Figure 3 we plot $m_i/m_t^* = H m_i/m_t$ as a function of x . This shows that for net erosion conditions all m_i increase with distance down slope and appear to increase at the same rate. The percentage contribution of each size class to the deposited layer is given by m_i/m_t which from (12) is equivalent to $v_i c_i / \sum_{i=1}^I v_i c_i$. Substituting for c_i from (15), we find

$$\frac{m_i}{m_t} = \frac{p_i v_i}{\sum_{i=1}^I p_i v_i}, \quad (26)$$

which is independent of x . Hence at steady state the percentage contributions of each size class in the deposited

Table 2. Hydraulic Parameters Assuming a Rectangular Rill

	$Q = 6 \text{ L min}^{-1}$		$Q = 9 \text{ L min}^{-1}$	
	$c_i(0) = 0$	$c_i(0) \neq 0$	$c_i(0) = 0$	$c_i(0) \neq 0$
h , cm	0.6	0.42	0.6	0.47
W_b , cm	8	10	10.5	12.5
$q = Q/W_b$, $\text{m}^2 \text{ s}^{-1}$	0.00125	0.001	0.00143	0.0012
Ω , W m^{-2}	0.86	0.69	0.98	0.82
γ , $\text{kg m}^{-2} \text{ s}^{-1}$	1.79	2.5	2.7	3.1
λ , $\text{kg m}^{-2} \text{ s}^{-1}$	0.011		0.028	
J^a , J kg^{-1}	4.8		2.80	
$F(\Omega - \Omega_{cr})^a$, W m^{-2}	0.053	0.051	0.079	0.071
F	0.062	0.075	0.081	0.087

^aFrom Polyakov and Nearing [2003].

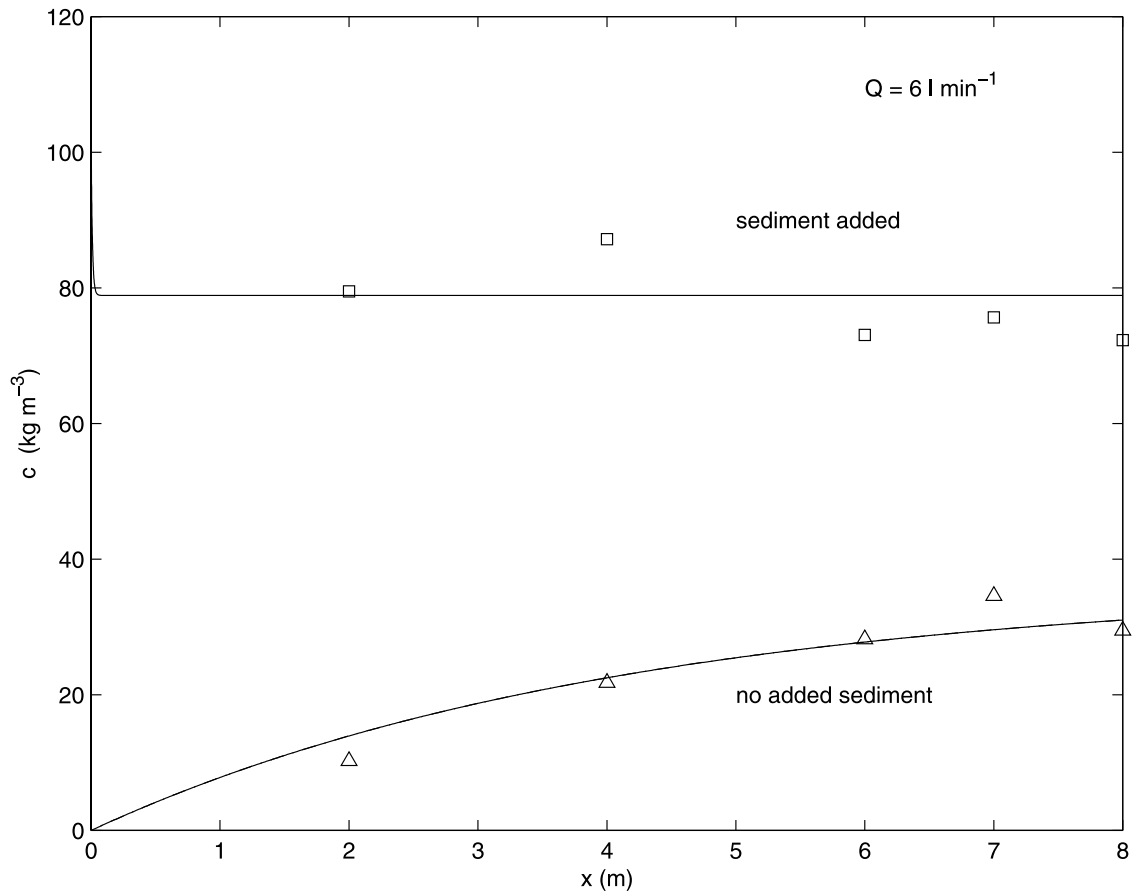


Figure 1. Measured (symbols) and predicted (lines) steady state total sediment concentration for sediment added and no added sediment for a rill flow rate of 6 L min⁻¹.

layer remain constant for all x . For the data in Figure 3, (26) gives m_i/m_t , $i = 1, 2, 3, 4$ and 5 as (0.03, 0.07, 0.34, 0.45, 0.11) which shows a significant coarsening of the sediment in the deposited layer compared to the p_i proportions of the original soil. A plot of m_i/m_t (not m_i/m_t^* as in Figure 3) is given in Figure 4 and shows that the percentage contributions of each size class to the deposited layer under net deposition conditions is quite different to those for net erosion conditions. First, they are not independent of x as shown by the region near $x = 0$ in Figure 4 where there are rapid changes. Second, the constant percentage contributions reached down slope are found from (20) and (22) as

$$\frac{m_i}{m_t} = \frac{v_i c_i}{\sum_{i=1}^I v_i c_i} = \frac{v_i c_i(0) [c_I(\infty)/c_I(0)]^{v_i/v_I}}{\sum_{i=1}^I v_i c_i(0) [c_I(\infty)/c_I(0)]^{v_i/v_I}}, \quad (27)$$

giving values of (0.07, 0.15, 0.41, 0.34, 0.03) for $i = 1, 2, 3, 4$ and 5. While these again demonstrate significant coarsening of the deposited layer, they are entirely different to those found from (26) for net erosion conditions. Thus both the makeup of the deposited layer and the suspended sediment concentration are different for both the net erosion and net deposition regimes and it is therefore not surprising that there is no unique value for the transport capacity for describing sediment transport under these two conditions.

[18] In the experiments of *Polyakov and Nearing* [2003], the flow widths and depths are different in the two cases of the added and the no added sediment discharge for the same flow rate, and it could therefore be postulated that this is a cause of the difference in transport capacity. We were able to show that this was definitely not the case, as even by keeping the hydraulic flow conditions the same, i.e., same depth, flow velocity and discharge for both net eroding and net deposition conditions, there remained the large difference in the calculated transport capacity between the two cases. This is also clear from the steady state analytical solutions for these two cases.

3.2. Limitations of the Transport Capacity Concept

[19] By modeling separately the erosion processes of deposition and entrainment, the Hairsine-Rose model yields different values for the transport capacity for the different flow conditions. Equation (18) shows that T_c for net erosion depends primarily on the settling velocities v_i and the proportions p_i of sediment in each size class, while T_c for net deposition, as shown by (23), depends on v_i and the incoming concentrations of each size class at $x = 0$. It is worth noting that the size class proportions of the original soil have no effect on net deposition T_c . This is due to the original soil being completely covered by the deposited layer whose composition is governed by both the size distribution of the inflowing sediment and the preferential

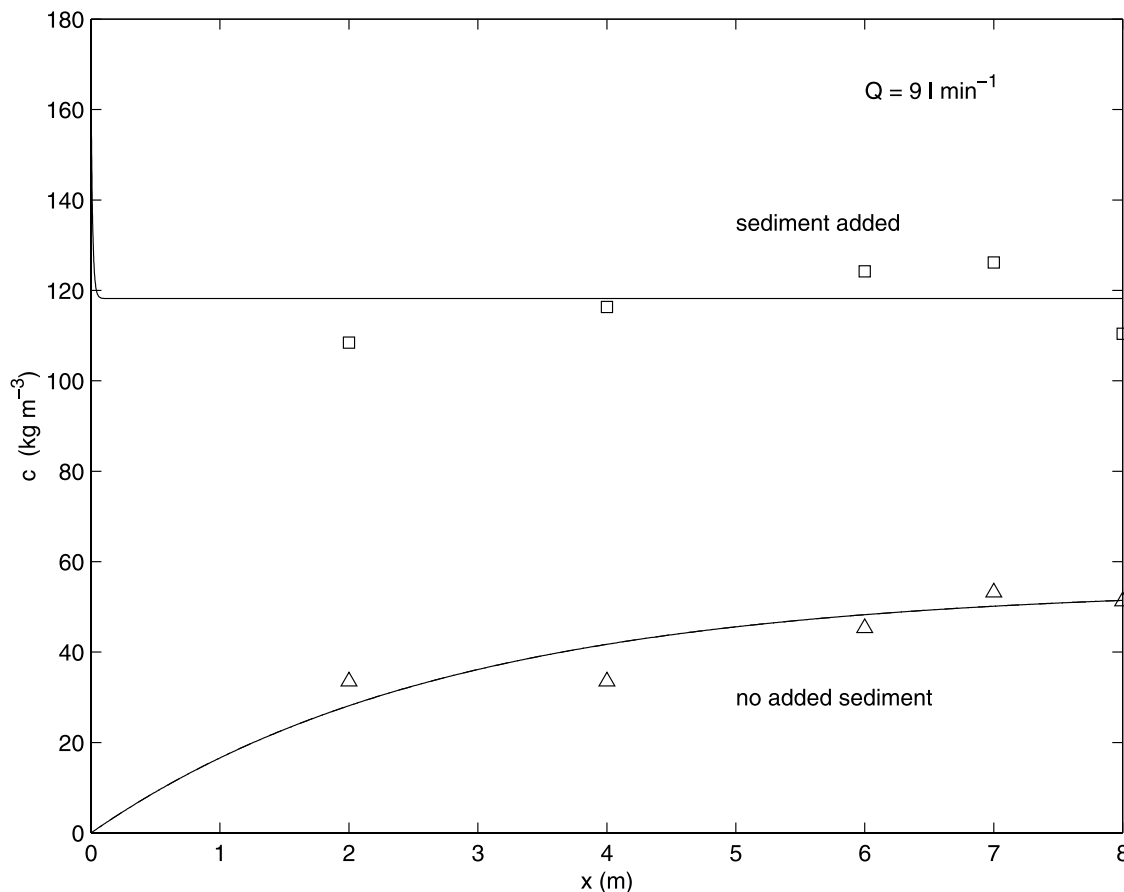


Figure 2. Measured (symbols) and predicted (lines) steady state total sediment concentration for sediment added and no added sediment for a rill flow rate of 9 L min^{-1} .

Table 3. Measured and Predicted Size Class Concentrations as a Function of Distance Down the Rill

Rill Length, m	Size Class i	$c_i(x)$ Net Erosion, kg m^{-3}		$c_i(x)$ Net Deposition, kg m^{-3}	
		Measured ^a	Predicted	Measured ^a	Predicted
<i>Discharge Q, 6 L min^{-1}</i>					
2	1	3.5	5.2	48.2	37.7
	2	2.8	3.3	15.8	22.0
	3	2.3	2.8	7.1	11.8
	4	2.0	2.3	7.1	6.8
	5	0.3	0.3	0.8	0.5
8	1	13.0	11.7	37.0	37.7
	2	6.4	7.3	17.4	22.2
	3	5.7	6.2	10.2	11.8
	4	4.5	5.2	7.3	6.8
	5	0.6	0.7	1.5	0.5
<i>Discharge Q, 9 L min^{-1}</i>					
2	1	13.4	10.6	66.5	60.5
	2	7.9	6.6	21.8	34.4
	3	5.9	5.6	8.7	15.2
	4	5.9	4.7	9.8	7.6
	5	1.4	0.7	3.3	0.4
8	1	15.5	19.3	49.2	60.5
	2	12.4	12.1	30.2	34.4
	3	10.4	10.3	17.9	15.2
	4	10.9	8.6	11.2	7.6
	5	2.1	1.2	2.2	0.4

^aFrom Polyakov and Nearing [2003].

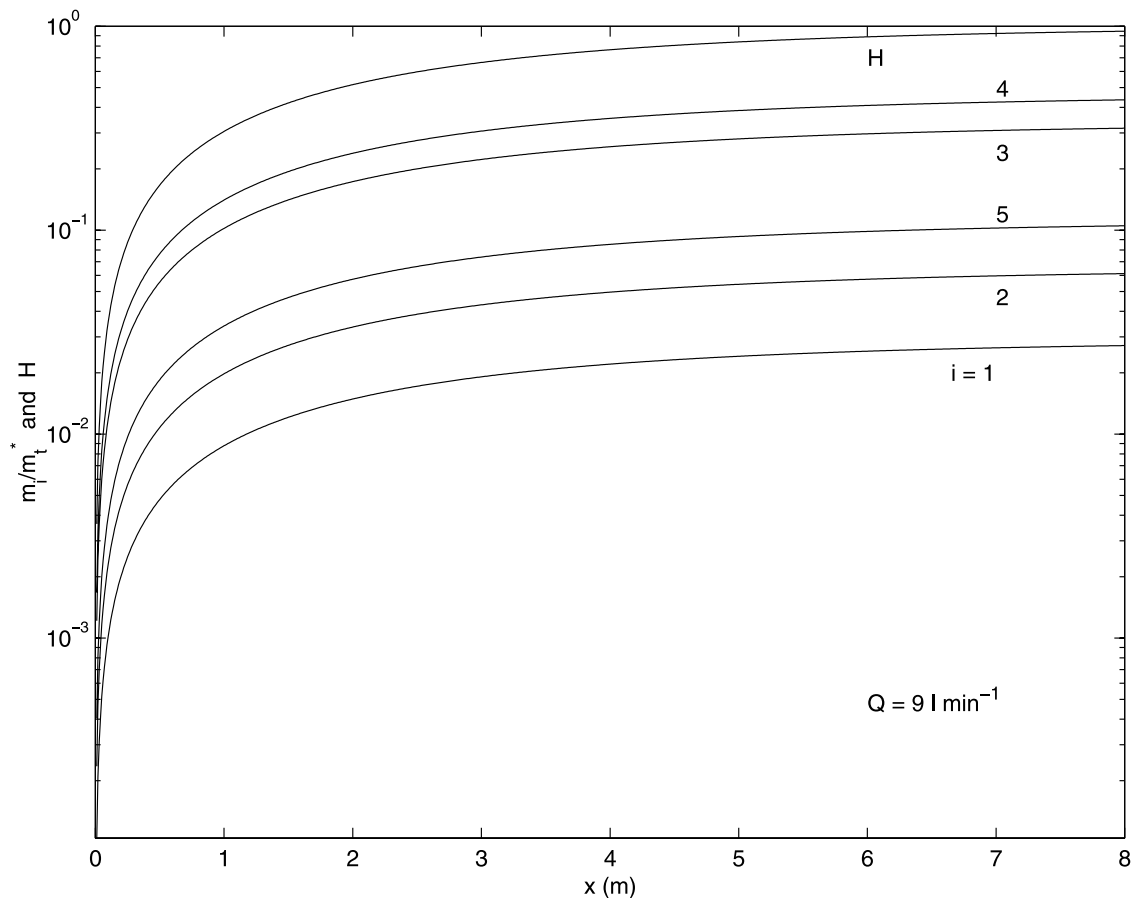


Figure 3. The mass of each size class in the deposited layer and its fraction of coverage H for the net erosion experiment with a rill discharge of 9 L min^{-1} .

depositional behavior of suspended sediment in the larger size classes. Second, the relationship between the size classes in suspension is again completely different for the two flow conditions. Under net erosion all the smaller size classes are directly proportional to the largest size class through (15) while for net deposition there is a power law dependence of the smaller classes on the largest size as expressed through (20). Third, we also see from Table 3 that under net deposition conditions there is considerable enrichment of the fine sediment in the overland flow. This perspective is consistent with the experiments of *Polyakov and Nearing* [2003] that show that T_c depends on erosion conditions.

[20] *Polyakov and Nearing* [2003, p. 39] discuss four possible explanations for the differences in measured T_c . These are “(i) sediment size differences due to preferential deposition of coarse sediment in the flow . . . , (ii) changes in hydraulic friction due to smoothing of the soil bed under a deposition regime, (iii) physical protection from detachment of soil from the rill bottom by moving bed load, or (iv) significantly less energy required to maintain the movement of the sediment in the flow compared to that required to detach new material from the soil bed.” While results in their Figure 4 suggest that reason ii was not a cause, the impact of the other explanations is not included in transport capacity-based erosion models. In contrast, the Hairsine-Rose model includes these effects and as such it has been able to reproduce the experimental data *Polyakov*

and Nearing [2003]. Effect i is included by using a multisize class erosion model and having deposition explicitly represented as a separate process. Explanations iii and iv are included through (5) which models the development of a covering layer of deposited sediment on top of the original soil. Owing to the effects of preferential deposition of coarse sediment, this layer has a different size distribution and cohesive strength to the original soil and it also provides it a percentage of protection H to the original soil as shown in Figure 3. Allowing for the different cohesive strength properties of the covering layer accounts directly for explanation iv. The development of such a layer has been clearly demonstrated through the experiments of *Heilig et al.* [2001]. Thus we conclude that the data and explanations offered by *Polyakov and Nearing* [2003] underscore the predictive potential of the form of the conceptual model adopted by *Hairsine and Rose* [1992a, 1992b] for modeling erosion due to shallow flows.

[21] It may also be possible that the difference of transport capacity observed in the experiments of *Polyakov and Nearing* [2003] could be due to a greater proportion of sediment of smaller size classes in the sediment added discharge. While this effect may be included in the experimental data, since inflowing size class information was not available, the incoming sediment concentrations used in the HR model were in direct proportion to the distribution of the original soil. Consequently, differences in outflowing concentrations between the net erosion and net

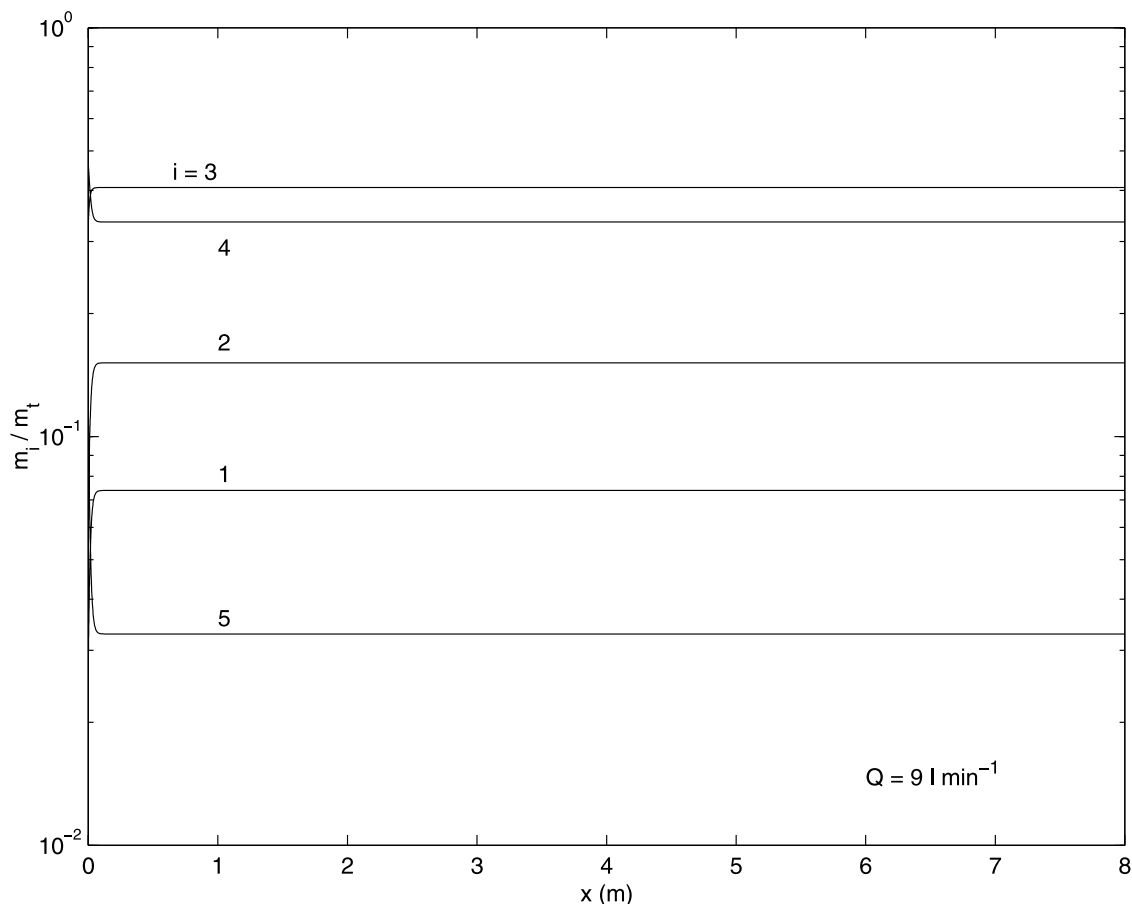


Figure 4. Fractional contribution of size classes in the deposited layer for the net deposition experiment with a rill discharge of 9 L min^{-1} .

deposition experiments are totally due to differences in the balance of erosion processes operating between the two experimental conditions. Under net erosion, entrainment of original soil still takes place as $H < 1$, hence equilibrium conditions result as a balance between three processes, i.e., entrainment of original soil, reentrainment of deposited soil and settling due to gravity. Under net deposition, the original soil makes no contribution to the steady state solution as it is completely covered by a deposited layer. Therefore equilibrium conditions result as a balance between only two processes, i.e., reentrainment of deposited soil and settling due to gravity.

[22] Polyakov and Nearing [2003, p. 42] note that widely used process-based models such as WEPP, LISEM and KINEROS2 allow for changes in transport capacity due to sediment sorting from deposition. They conclude however that their data suggests “that this is not the only, nor even the primary, mechanism to account for the large observed differences in sediment load” between net erosion and net deposition regimes. This statement supports modeling erosion mechanisms as separate processes, rather than using the transport capacity since with this concept the effect of the sediment size distribution cannot be deduced, but rather must be imposed by some means, e.g., calibration. In the Hairsine-Rose model, all the large observed differences in

sediment load between the two regimes can be fully accounted for.

[23] Difficulties with the suitability of the transport capacity concept have been previously raised by Huang *et al.* [1996, 1999]. The experiments of Huang *et al.* [1999] demonstrated that the transport capacity depends on the sediment transport conditions and they concluded that “instead of fitting a preconceived detachment limiting/transport limiting process regime, the most logical approach seems to be the [Hairsine-] Rose model concept.” The present analysis provides further evidence supporting this conclusion.

3.3. Transport Capacity for Single Size Class Soils

[24] For soils composed of a single size class with fall velocity v_1 , the transport capacity for net erosion is given from (18) as $T_c = q\gamma/v_1$. For net deposition regimes, the transport capacity as found from (23) and (24) also reduces to $T_c = q\gamma/v_1$. Thus it is only for single sized class soils that the transport capacity is truly unique.

4. Conclusions

[25] The rates of entrainment, reentrainment and deposition are continuous dynamic processes which occur simultaneously through an erosion event. The nature of these dynamic processes does not change as flow conditions

move from net erosion to net deposition. Conditions of net erosion and net deposition are merely a change in the balance of these rates. The use of a prescribed transport capacity (T_c) in erosion models requires different rate equations to describe different aspects of the same physical process and is therefore physically inconsistent. Transport capacity for any particular flow conditions evolves from the flow itself and is merely given by a net zero balance across all erosion processes; it is an outcome of the erosion process and not an input to the process. A physically consistent model of soil erosion therefore requires only one set of rate equations which should predict sediment transport in both sets of conditions. Currently, the only such physically consistent model is that given by *Hairsine and Rose* [1992a] and as shown here it is capable of reproducing and explaining the observed sediment transport under both the net erosion and net deposition experiments of *Polyakov and Nearing* [2003].

References

- Beasley, D. B., L. F. Huggins, and E. J. Monke (1980), ANSWERS—A model for watershed planning, *Trans. Am. Soc. Agric. Eng.*, **23**, 938–944.
- Beuselinck, L., G. Govers, P. B. Hairsine, G. C. Sander, and M. Breynaert (2002a), The influence of rainfall on sediment transport by overland flow over areas of net deposition, *J. Hydrol.*, **257**, 145–163.
- Beuselinck, L., P. B. Hairsine, G. Govers, and J. Poesen (2002b), Evaluating a single-class net deposition equation in overland flow conditions, *Water Resour. Res.*, **38**(7), 1110, doi:10.1029/2001WR000248.
- Cheng, N. (1997), Simplified settling velocity formula for sediment particle, *J. Hydraul. Eng.*, **123**, 149–152.
- De Roo, A. P. J., C. G. Wesseling, and C. J. Ritsema (1996), LISEM: A single-event physically based hydrological and soil erosion model for drainage basins: I. Theory, input and output, *Hydrol. Processes*, **10**, 1107–1117.
- Hairsine, P. B., and C. W. Rose (1992a), Modeling water erosion due to overland flow using physical principles: 1. Sheet flow, *Water Resour. Res.*, **28**, 237–243.
- Hairsine, P. B., and C. W. Rose (1992b), Modeling water erosion due to overland flow using physical principles: 2. Rill flow, *Water Resour. Res.*, **28**, 245–250.
- Hairsine, P. B., L. Beuselinck, and G. C. Sander (2002), Sediment transport through an area of net deposition, *Water Resour. Res.*, **38**(6), 1086, doi:10.1029/2001WR000265.
- Heilig, A., D. DeBruyn, M. T. Walker, C. W. Rose, J.-Y. Parlange, T. S. Steenhuis, G. C. Sander, P. B. Hairsine, W. L. Hogarth, and L. P. Walker (2001), Testing a mechanistic soil erosion model with a simple experiment, *J. Hydrol.*, **244**, 9–16.
- Huang, C., J. M. Bradford, and J. M. Lafren (1996), Evaluation of the detachment-transport coupling concept in the WEPP rill erosion equation, *Soil Sci. Soc. Am. J.*, **60**, 734–739.
- Huang, C., L. K. Wells, and L. D. Norton (1999), Sediment transport capacity and erosion processes: Model concepts and reality, *Earth Surf. Processes Landforms*, **24**, 503–516.
- Morgan, R. P. C., J. N. Quinton, R. E. Smith, G. Govers, J. W. A. Poesen, K. Auerswald, G. Chisci, D. Torri, and M. E. Styczen (1998), The European Soil Erosion Model (EUROSEM): A dynamic approach for predicting sediment transport from fields and small catchments, *Earth Surf. Processes Landforms*, **23**, 527–544.
- Nearing, M. A., G. R. Foster, L. J. Lane, and S. C. Finkner (1989), A process based soil erosion model for USDA water erosion prediction project technology, *Trans. Am. Soc. Agric. Eng.*, **32**, 1587–1593.
- Polyakov, V. O., and M. A. Nearing (2003), Sediment transport in rill flow under deposition and detachment conditions, *Catena*, **51**, 33–43.
- Proffitt, A. P. B., P. B. Hairsine, and C. W. Rose (1993), Modelling soil erosion by overland flow: Application over a range of hydraulic conditions, *Trans. Am. Soc. Agric. Eng.*, **36**, 1743–1753.
- Sander, G. C., P. B. Hairsine, C. W. Rose, D. Cassidy, J. Y. Parlange, W. L. Hogarth, and I. Lisle (1996), Unsteady soil erosion model, analytical solutions and comparison with experimental results, *J. Hydrol.*, **178**, 351–367.
- Sander, G. C., P. B. Hairsine, L. Beuselinck, and G. Govers (2002), Steady state sediment transport through an area of net deposition: Multisize class solutions, *Water Resour. Res.*, **38**(6), 1087, doi:10.1029/2001WR000323.
- Woolhiser, D. A., R. E. Smith, and D. C. Goodrich (1990), KINEROS, A kinematic runoff and erosion model: Documentation and user manual, *Rep. ARS-77*, Agric. Res. Serv., U.S. Dep. of Agric., Washington, D. C.

D. A. Barry and M. B. Parlange, School of Architecture, Civil and Environmental Engineering, Ecole Polytechnique Fédérale de Lausanne, CH-1015 Lausanne, Switzerland. (andrew.barry@epfl.ch; marc.parlange@epfl.ch)

W. L. Hogarth, Faculty of Science and Information Technology, University of Newcastle, Newcastle, N. S. W. 2308, Australia. (bill.hogarth@newcastle.edu.au)

J.-Y. Parlange, Department of Biological and Environmental Engineering, Cornell University, Ithaca, NY 14853-5701, USA. (jp58@cornell.edu)

G. C. Sander, Department of Civil and Building Engineering, Loughborough University, Loughborough LE11 3TU, UK. (g.sander@lboro.ac.uk)